

# GRAPHENE OXIDE AND A GO/ZnO NANOCOMPOSITE AS CATALYSTS FOR EPOXY RING-OPENING OF EPOXIDIZED SOYBEAN FATTY ACIDS METHYL ESTERS

Kaline A. Wanderley<sup>1</sup>, Amanda M. Leite<sup>2</sup>, Gabriel Cardoso<sup>2</sup>, Anderson M. Medeiros<sup>1</sup>,  
Caroline L. Matos<sup>1</sup>, Romulo C. Dutra<sup>1</sup> and Paulo A. Z. Suarez<sup>1\*</sup>

<sup>1</sup> Universidade de Brasília, Instituto de Química, Laboratório de Materiais e Combustíveis, Brasília, DF, Brasil.  
ORCID: 0000-0002-3223-4501; E-mail: psuarez@unb.br - ORCID: 0000-0002-1195-3128

<sup>2</sup> Universidade de Brasília, Instituto de Química, Laboratório de Inorgânica e Materiais, Brasília, DF, Brasil.

(Submitted: November 12, 2018 ; Revised: January 21, 2019 ; Accepted: January 21, 2019)

**Abstract** - In this work, the grapheme oxide (GO) and GO/ZnO nanocomposite were successfully obtained from the oxidation of graphite and characterized by X-ray diffraction (XRD), scanning electron microscopy (SEM), transmission electron microscopy (TEM), and thermogravimetric analysis (TGA). In the GO/ZnO nanocomposite, the GO sheets were coated with aggregated ZnO nanoneedles with *ca.* 20 nm of diameter. The obtained materials were used as heterogeneous catalysts for acetylation of Soybean Fatty Acids Methyl Esters (FAME), promoting the epoxy ring-opening using acetic anhydride. The epoxy ring was almost completely opened in the presence of GO or GO/ZnO nanocomposites, with conversion rates up to 99% and selectivity of *ca.* 90%, and partially opened using only ZnO. The GO/Zn and GO catalysts were reused three times with conversion rates of *ca.* 85 and 74%, respectively.

**Keywords:** Graphene oxide; ZnO; Nanocomposite; Epoxide ring-opening; Acetylation.

## INTRODUCTION

Graphene oxide (GO) and related materials such as graphene/metal oxide composites have received great attention due to their low cost, easy obtainability and compatibility with various substrates (Nie et al., 2016; Sakthivel et al., 2017). Also, synergistic effects provided by the combination of metal oxides and graphene can improve their catalytic performance compared to the individual metal oxides (Nie et al., 2016; Sakthivel et al., 2017). Among these, particularly ZnO (Guo et al., 2016; Nasrollahzadeh et al., 2014) has excelled because of its strong oxidizing power, non-toxic nature, low cost and its catalytic ability in both acidic and basic medium (Huang et al., 2012; Joonwchien et al., 2012).

One of the ways most widely used to obtain GO is through the Hummers method (Hummers and

Offeman, 1958), which is based on the exhaustive oxidation of graphite under strong acid conditions, using concentrated sulfuric acid, permanganate and hydrogen peroxide. In the synthesis of GO by the Hummers method, a series of functional groups containing oxygen, such as alcohols, epoxides and carboxylates, as well as a small quantity of sulfate groups, are introduced to the graphene plane, acting, thus, as Brønsted acids (Wang, et al., 2013), making these materials very active as catalysts in a myriad of organic molecule transformations (Navalón et al., 2018). Moreover, GO/metal oxide composites have the advantage of having both strong Brønsted as well as Lewis acid properties (Marso et al., 2017). Thus, the introduction of different functional groups makes GO and its composites excellent catalysts for many synthetic transformations, such as sulfide, thiol

\* Corresponding author: Paulo A. Z. Suarez - E-mail: psuarez@unb.br

(Dreyer et al., 2010), C-H bond (Jia et al., 2011), alcohol and alkene oxidation (Dreyer et al., 2010), hydrogenation of nitrobenzene (Gao et al., 2011) and epoxide ring opening (Acocella et al., 2016; Dhakshinamoorthy et al., 2012). These solid materials can act as heterogeneous acid catalysts, which prevent the dispersion in water, enhance the mechanical properties and interact easily with nucleophilic centers (Cheng et al., 2016; Garg et al., 2014).

Epoxidation followed by a ring-opening reaction, particularly of vegetable oils or Fatty Acids Methyl Esters (FAME), has been studied with the intent of utilizing the epoxidized products as intermediates for polymer preparations (Diciccio and Coates, 2011; Nicolau et al., 2012), such as polyesters, polyurethanes, biolubricants (Sharma et al., 2015; Sharma and Dalai, 2013), and epoxy resins (Samper et al., 2012), or as stabilizer for plastics. FAME, produced from many different sources (Ruschel et al., 2016), have been used as biofuel (biodiesel) to partially or completely substitute diesel fuel. Because of the poor low temperature performance, and low oxidative and thermal stability of some vegetable oils and their derived FAME, epoxidation was also suggested to improve these undesired properties (Biresaw and Bantchev, 2013; Wang et al., 2013).

After the vegetable oil or FAME is epoxidized, the first modification step performed is the oxirane ring-opening, followed by an acylation step. Recent studies have shown that ring-opening, esterification and/or acetylation result in: *i*) improved viscosity index; *ii*) better low temperature flow properties; *iii*) increased thermal and oxidative stability; *iv*) lower coefficients of friction, and *v*) enhanced lubricity characteristics (McNutt and He, 2016). Nevertheless, epoxy ring-opening, using acetic anhydride, is performed with strong acid or basic catalysts, excess of reagents, high temperatures, and long times, as well as high mass fractions of heterogeneous catalysts. In this context, the relatively acid catalysts GO and GO/ZnO were used in the ring-opening reaction of epoxidized soybean FAME.

## EXPERIMENTAL SECTION

### Chemicals and Materials

Synthetic graphite powder (< 20 micron), zinc oxide (ZnO), anhydrous MgSO<sub>4</sub> and basic alumina (Al<sub>2</sub>O<sub>3</sub>) were purchased from Aldrich; potassium permanganate (KMnO<sub>4</sub>) from Merck; 98% sulfuric acid (H<sub>2</sub>SO<sub>4</sub>), 30% hydrogen peroxide (H<sub>2</sub>O<sub>2</sub>), zinc chloride (ZnCl<sub>2</sub>), sodium hydroxide (NaOH), acetic anhydride, and absolute ethanol were purchased from Vetec. Commercial refined soybean oil was purchased from a local store. 99% methanol (MeOH) was purchased from Cromaline. Potassium hydroxide

(KOH) and sodium bicarbonate (NaHCO<sub>3</sub>) were purchased from Synth. 85% Formic acid (HCOOH) was purchased from Dinâmica and the Nitrogen Gas (N<sub>2</sub>) was purchased from White Martins. All chemicals were analytical grade and were used as received without further purification.

### Synthesis of Graphene Oxide (GO) and GO/ZnO Nanocomposite

The graphene oxide (GO) was prepared from graphite powder using a modified (Huang et al., 2012; Min and Lu, 2011) Hummers method (Hummers and Offeman, 1958). H<sub>2</sub>SO<sub>4</sub> (46 mL) and graphite (2 g) were stirred vigorously in an ice bath, KMnO<sub>4</sub> (6 g) was slowly added and stirred for about 30 min. Water (50 mL) was added and stirred. Finally, more water (300 mL) was added, followed by the slow addition of H<sub>2</sub>O<sub>2</sub> (10 mL). The dispersion obtained was centrifuged at 6000 rpm for 15 min and rinsed repeatedly with water to remove the remaining salt until pH 7, washed with ethanol and dried at room temperature (Zhang et al., 2011).

The synthesis of GO/ZnO nanocomposite was based on Li et al. (2012), in which 0.1 g of GO was dispersed in 40 mL of water by ultra-sonication. ZnCl<sub>2</sub> (1.0 mmol) and NaOH (10.0 mmol) were successively dissolved in the GO suspension. The mixture was stirred for 6h at 90 °C and then cooled to room temperature. The composite obtained was filtered, washed with water and ethanol, and dried at room temperature.

### FAME Epoxidation and Ring-Opening Reactions

The soybean FAME was obtained by transesterification, as described in the literature (Oliveira et al., 2006; Ramalho et al., 2014), with a mass ratio of 6.42:57.5:1 (soybean oil:MeOH:KOH), in which KOH was completely dissolved in MeOH under magnetic stirring and nitrogen atmosphere in a reactor. Then, the dried soybean oil was added into the reactor and the mixture was maintained under stirring for 3 h at room temperature. The final product was washed repeatedly with distilled water, dried with anhydrous MgSO<sub>4</sub> under vacuum, filtered on a basic alumina column under nitrogen atmosphere and stored at below 0 °C, to prevent the oxidation of the unsaturation.

Soybean FAME (*ca.* 30 g) was placed in a reflux system at 60 °C and a mixture of H<sub>2</sub>O<sub>2</sub> and formic acid was slowly added to the reaction, with a mass ratio of 1.42:1.92:1.88 (Soybean FAME:Formic Acid:Hydrogen Peroxide); then the temperature of the system was increased to 80 °C and the reaction refluxed for 5 h. After cooling, the system was washed repeatedly with distilled water, dried with anhydrous MgSO<sub>4</sub> under vacuum, filtered on a basic alumina

column under nitrogen atmosphere and stored at below 0 °C (Campanella et al., 2008).

After the FAME epoxidation, the oxirane ring opening was performed by acetylation reaction (Oliveira et al., 2017), in which FAME epoxide (1,0 g) was mixed with acetic anhydride (1,0 g) and different amounts of GO, ZnO and GO/ZnO catalysts were added to the mixture under stirring in a Schlenk tube at 120 °C for 12 h or 24 h. The modified FAME was washed with ethanol and centrifuged at 6000 rpm for 15 min, then dried under vacuum for 24 h. The reusability of GO and GO/ZnO catalysts was measured in the oxirane ring-opening of epoxidized soybean FAME; three cycles of the catalytic experiment for each catalyst were carried out in optimal conditions. In all recycling experiments, the reaction mixture was centrifuged after the reaction in order to separate the catalysts. The GO and GO/ZnO catalysts were washed with water and dried at 50 °C before being reused in the reaction.

### General Characterization

GO and GO/ZnO nanocomposites were characterized by X-ray powder diffraction collected at room temperature using a Bruker D8 with copper rotating anode ( $\lambda_{\text{CuK}\alpha 1} = 1.5404 \text{ \AA}$ ,  $\lambda_{\text{CuK}\alpha 2} = 1.5444 \text{ \AA}$ ,  $I_{02}/I_{01} = 0.5$ ) sealed-tube fine focus X-ray source. Intensity data were collected in step scanning mode ranging from 5 to 90° (2 $\theta$ ), step size of 0.01°, Soller slit with 2.5° divergence, scattering slit of 2.5° and receiving slit of 0.3 mm. Scanning Electron Microscopy (SEM) images were collected using a JEOL scanning electron microscope (JSM-6610) working at 15 kV. Samples were prepared by deposition on aluminum sample holders followed by carbon coating and a later gold coating (*ca.* 20 nm) to 5 mA. Transmission Electron Microscopy (TEM) images were obtained using a JEOL 1011 transmission electron microscope. Samples were diluted in ethanol, deposited on a copper grid, and dried at room temperature. The FAME products were analyzed by infrared spectroscopy using a FT-IR spectrometer model IR Prestige from Shimadzu, with ATR Miracle cell and by <sup>1</sup>H nuclear magnetic resonance spectroscopy (600 MHz, CDCl<sub>3</sub>), using a Bruker, model Magneto Ascend 600 with Console Avance III HD.

## RESULTS AND DISCUSSION

### Characterization of GO and GO/ZnO Nanocomposites

Oxidation of graphite to graphene using a modified Hummers method was evaluated by X-ray diffraction (XRD). The XRD patterns (Figure 1) show that after oxidation, the diffraction peaks of graphite in 2 $\theta$  = 26.6° ( $d_{\text{hkl}} = 002$ ) and 2 $\theta$  = 54.4° ( $d_{\text{hkl}} = 004$ ) disappeared,

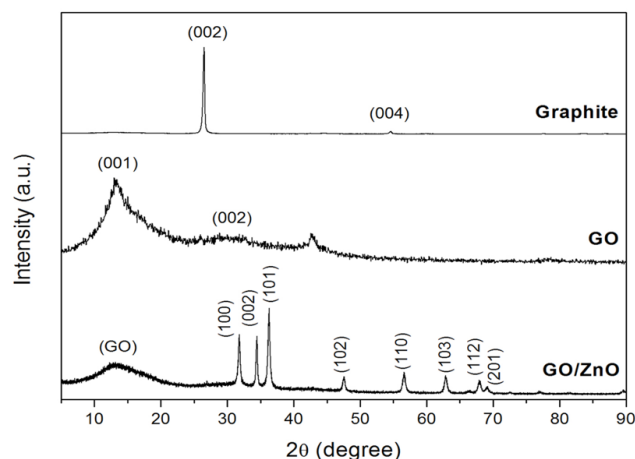


**Figure 1.** XRD Patterns of graphite, graphene oxide (GO) and GO/ZnO nanocomposite.

while for graphene a broad and characteristic peak appeared at a lower diffraction angle in 2 $\theta$  = 13.1° ( $d_{\text{hkl}} = 001$ ). The absence of the characteristic diffraction peaks of graphite confirmed the obtainment of graphene oxide (Huang et al., 2012). Moreover, the introduction of oxygen-containing functional groups on the surfaces of the graphite sheet induced an interplanar distance in GO of *ca.* 6.75 Å, using Bragg's law ( $2d \sin \theta = n\lambda$ ) (Sheng et al., 2013), that is much larger than of graphite (3.35 Å), as described in the literature (Bian et al., 2009a; Bian et al., 2009b). The diffraction peaks of the GO/ZnO nanocomposite are like those of hexagonal phase wurtzite ZnO (data\_82028-ICSD); as well the characteristic diffraction peak of graphene was observed in 2 $\theta$  = 13.1° ( $d_{\text{hkl}} = 001$ ), demonstrating that the GO/ZnO nanocomposite was obtained successfully.

Microstructures and morphologies of GO and the GO/ZnO nanocomposite were evaluated by scanning electron microscopy (SEM) and transmission electron microscopy (TEM). In the SEM image of GO (Figure 2), the stacked structure of graphene sheets can be seen with thin layers arranged like waves or wrinkles in the surface, whereas for the GO/ZnO nanocomposite the presence is observed of small particles of ZnO deposited on and between the GO sheet surfaces, as can be best seen in the TEM images (Figure 3).

In the TEM and HR-TEM images (Figure 3) it is possible to distinguish the light-gray thin films, that are the GO sheets, from the dark regions on the

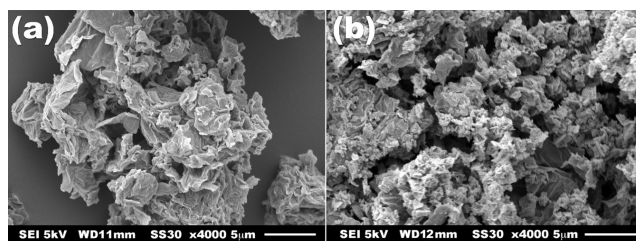


**Figure 2.** SEM images of (a) GO and (b) GO/ZnO nanocomposite.

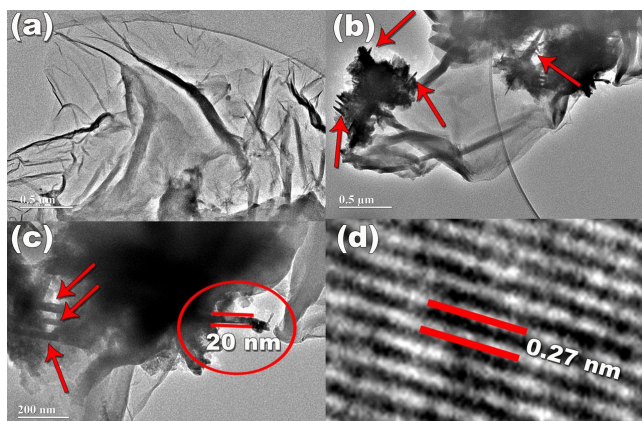


**Figure 3.** HR-TEM images of (a) GO, (b) GO/ZnO, (c) ZnO nanoneedles are indicated by red arrows and (d) interplanar distance of ZnO nanoparticle.

GO background that are due to the presence of ZnO nanoparticles. The GO sheets were decorated with aggregated ZnO nanoneedles with *ca.* 20 nm of diameter, in which the ZnO nanoparticles were mainly located at the edge of the GO sheets. The interplanar distance found in the HR-TEM was *ca.* 0.272 nm, which corroborates with data of interplanar spacing of ZnO obtained by the XRD pattern of *ca.* 2.47 Å, using Bragg's law ( $2d \sin \theta = \lambda$ ) in  $2\theta = 36.31^\circ$  ( $d_{hkl} = 101$ ), Figure 1.

Thermogravimetric curves show the thermal stability of GO and GO/ZnO (Figure 4). The highest rate of mass loss of GO occurred between 100 and 300 °C, indicating the release of CO, CO<sub>2</sub> and vapors from the most labile functional groups during pyrolysis. The differential thermal analysis (DTA) curve of GO/ZnO presents an exothermic loss due to liberation of CO, CO<sub>2</sub> and vapors due to the presence of GO in the nanocomposite. At higher temperatures, weight loss continues up to 500 °C, which could be associated to decomposition of reminiscent Zn(OH)<sub>2</sub> (Moharram et al., 2014). Above 700 °C, the DTA curve of GO/ZnO has a prominent endothermic peak which can be attributed to the structural reorganization of ZnO, reduction and sublimation of the Zn (Anthrop and Searcy, 1964), and the crystallization of some amorphous carbon (Araújo et al., 2009). These results agree with XRD pattern data, confirming the obtaining of the nanocomposite and, moreover, showing their thermal stability.

### Catalytic Performance of GO and GO/ZnO nanocomposite

Soybean FAME were obtained by transesterification as described in a previous work (Ramalho et al., 2014), using KOH, methanol and dried soybean oil. The final product was *ca.* 99.3% pure in FAME, measured by HPLC using a method previously described (Carvalho

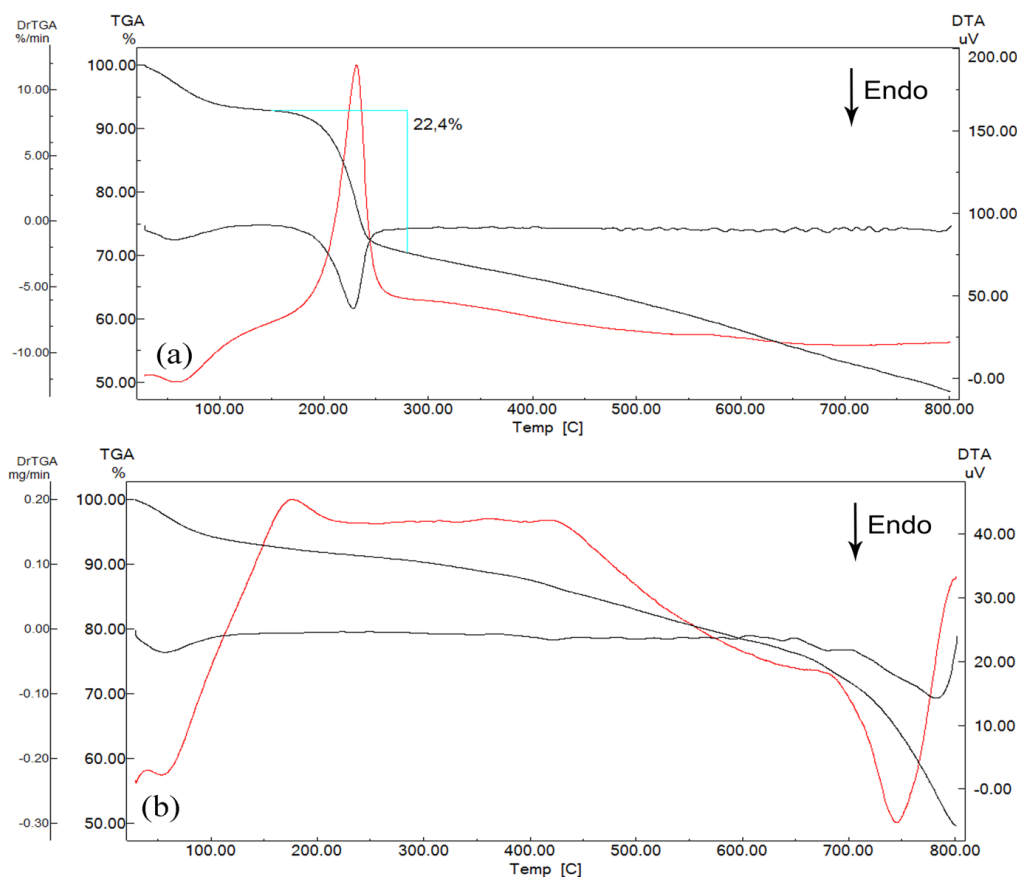


**Figure 4.** Thermogravimetric curves of (a) GO and (b) GO/ZnO.

et al., 2012). Moreover, soybean FAME and epoxide soybean FAME were evaluated by FTIR and  $^1\text{H}$  NMR spectroscopies (Figure 5). The main characteristic of the soybean FAME in the FTIR spectrum is the presence of an absorption band attributed to  $\text{sp}^2$  C-H groups with a stretch at  $3010\text{ cm}^{-1}$ . There are characteristic peaks in the  $^1\text{H}$  NMR spectrum with chemical shifts in the region of 5.2 - 5.6 ppm (Y in Figure 5b), which are attributed to the hydrogens adjacent to the unsaturation.

When the epoxide soybean FAME is formed, the characteristic band in the FTIR spectrum of  $\text{sp}^2$  C-H of the FAME disappears and new ones arise at *ca.* 823 and  $842\text{ cm}^{-1}$  referring to C-O stretches present in the oxirane ring of the epoxy group. The  $^1\text{H}$  NMR spectrum shows that the typical signals of the hydrogen adjacent to the FAME unsaturation bond at 5.2 - 5.6 ppm (Y in Figure 5b) vanished. Concomitantly, the hydrogen signals of the epoxide ring arose between 2.8 - 3.2 ppm, Z in Figure 5b (Jacintho et al., 2009; Oliveira et al., 2017). The conversion of soybean FAME to epoxide soybean FAME ( $(Y_{\text{initial}} - Y_{\text{final}})/Y_{\text{initial}} \times 100$ ) was *ca.* 98.4% and the selectivity of the epoxidation reaction ( $Z/Y \times 100$ ) was *ca.* 79.8%, because the 2H of Y form 2H of Z, in which Y is the amount of hydrogen in the peak area from 5.2 - 5.6 ppm and Z is the amount of unshielded hydrogen in the peak area

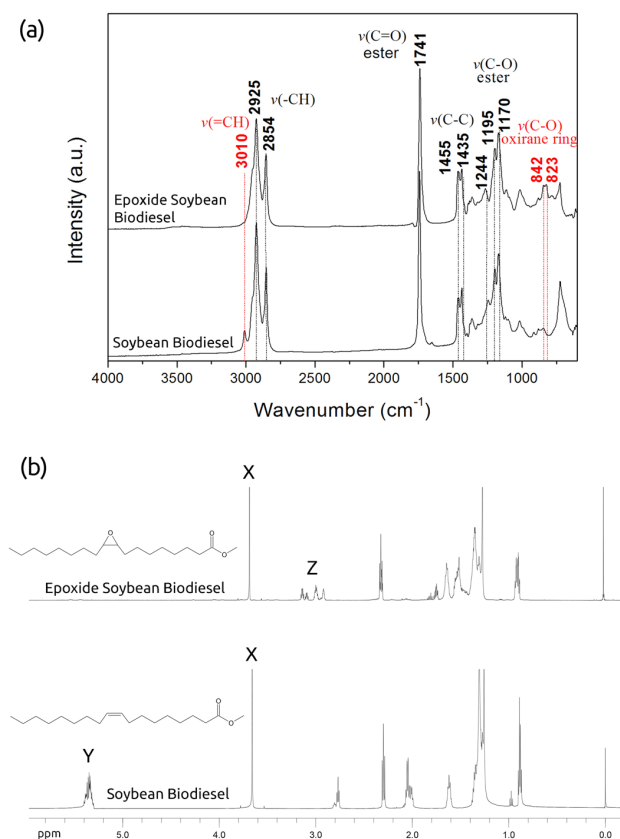


**Figure 5.** (a) FTIR and (b)  $^1\text{H}$  NMR spectra of the soybean FAME and epoxidized soybean FAME.

from 2.8 - 3.2 ppm. According to the literature, it is possible to identify the opening of the epoxide by the integration of the relative areas in  $^1\text{H}$  MNR spectra (Aerts and Jacobs, 2004). The peak at *ca.* 3.6 ppm (X in Figure 5b), corresponding to  $\text{OCH}_3$  hydrogens of the terminal ester groups of the FAME carbon chain, was used as internal standard for conversion and selectivity calculation, since it does not change in the reaction.

The epoxidation was performed aiming at posterior epoxy ring-opening with acetic anhydride in the presence of GO and GO/ZnO catalysts, resulting in an acetylated FAME, the di-acetyl soybean FAME (Figure 6). The acetylation products were analyzed by FTIR and  $^1\text{H}$  NMR spectroscopies.

The disappearance of characteristic vibrational modes of epoxy at *ca.* 823 and  $842\text{ cm}^{-1}$  in the FTIR spectrum (Figure 7) evidences the oxirane ring-opening, as well as the absorption band at *ca.*  $1234\text{ cm}^{-1}$  related to the acetyl groups present in the structure (Azeh et al., 2013; Wang et al., 2016). Another important indication of the addition of acetic anhydride in the modified FAME is the presence of the vibrational mode at *ca.*  $1738\text{ cm}^{-1}$  related to C=O stretches.

The epoxy ring-opening reaction was evaluated by  $^1\text{H}$  NMR spectroscopy by the decrease of the characteristic peaks of the protons adjacent to the oxirane ring at *ca.* 2.8 at 3.2 ppm (Scala and Wool, 2002) (Figure 8). The conversion of the epoxy ring-opening reaction was calculated, as before, using the relation  $(Z_{\text{initial}} - Z_{\text{final}})/Z_{\text{initial}} \times 100$  and the selectivity of the acetylation reaction by  $A/3Z \times 100$ , since the 2H of Z form 6H of A (Figure 8), an unshielded methyl adjacent to a carbonyl of the di-acetyl group, in which A is the amount of hydrogen in the peak area around 2.0 ppm and Z is the amount of unshielded hydrogen in the peak area from 2.8 - 3.2 ppm. Thus, the peak at

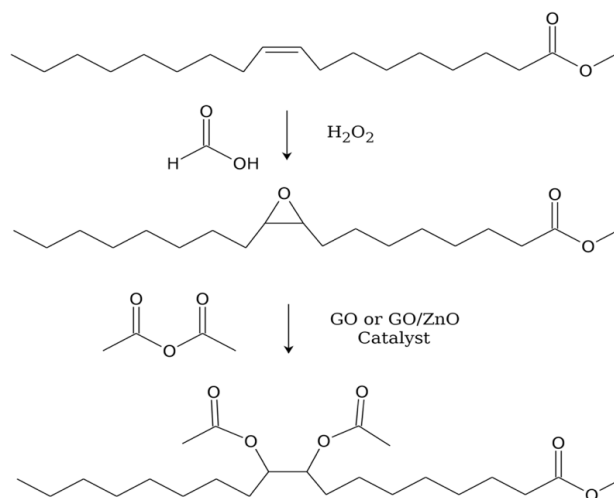


**Figure 6.** Epoxidation and ring-opening of epoxidized soybean FAME.

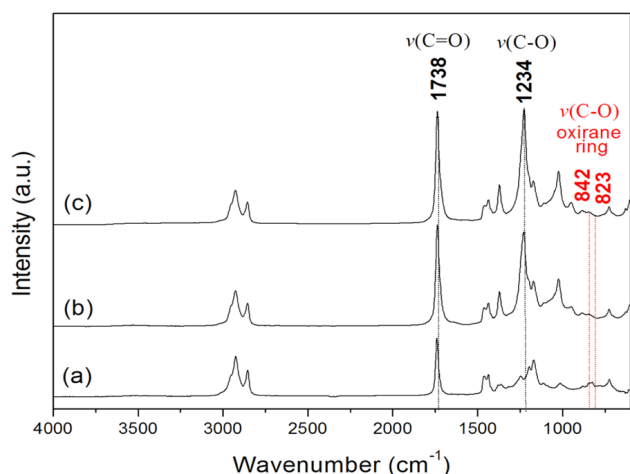


**Figure 7.** FTIR Spectra of (a) Epoxide Soybean FAME and oxirane ring-opening reaction of the epoxidized soybean FAME performed with acetic anhydride in the presence of (b) GO and (c) GO/ZnO catalysts.

*ca.* 3.6 ppm (X in Figure 8), corresponding to  $\text{OCH}_3$  hydrogens of the terminal ester groups of the FAME carbon chain, was also used as internal standard, because to it does not change during the reaction.

Acetic anhydride represents a relatively weak nucleophile. Therefore, the reaction usually demands high acidity/alkalinity, excess reagent, or long reaction times and high temperatures (Madankar et al., 2013). The GO and GO/ZnO catalysts were thermally stable around 150 °C (Figure 4); thus, the acetylation reaction was performed at 120 °C and 12 or 24 h using 1 or 10 % w/w of catalysts (Table 1). Reactions carried out at lower temperatures (80 °C or 100 °C) and for a short time (until 12 h) present low conversion yields (*ca.* 30 to 45%). The epoxy ring was almost completely open in the presence of GO/ZnO nanocomposite catalyst (*ca.* 98.6%), partially open using only GO (*ca.* 88.2%), and poorly opened using only ZnO (*ca.* 59.6%) as catalysts, at optimal conditions, at 120 °C for 24 h. The selectivity was increased when the amount of catalyst was enhanced to 10% w/w, being still a low amount of catalyst, mainly ZnO in the GO/ZnO nanocomposite, comparing with works in the literature with similar results using 15% w/w of catalyst for epoxy ring-opening in the acetylation reaction (Oliveira et al., 2017). The results are even better when the amount of GO was enhanced to 20% w/w, showing the efficiency of GO as acid catalyst.

### Catalytic Recycle

The reusability of GO and GO/ZnO nanocomposite catalysts were performed in the epoxy ring-opening of epoxidized FAME (Figure 9), showing activities up to 85% in all recycle reactions. There was a small mass loss, but after three cycles the catalytic activity was almost completely preserved. XRD analysis (Figure 9b) indicates the leaching of the ZnO nanoparticles

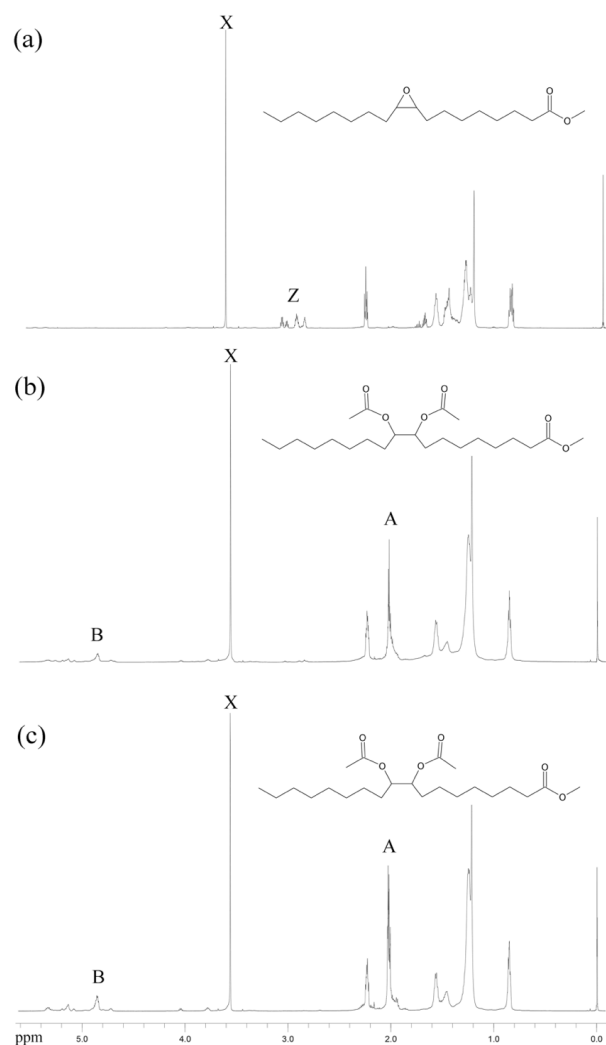


**Figure 8.**  $^1\text{H}$  MNR spectra of (a) Epoxide Soybean FAME and oxirane ring-opening reaction of the epoxidized FAME performed with acetic anhydride in the presence of (b) GO and (c) GO/ZnO catalysts.

**Table 1.** Conversion and selectivity of epoxy ring-opening in the acetylation reaction, in the presence of GO, ZnO and GO/ZnO catalysts at 120 °C for different times and amounts of catalysts.

Catalyst	% w/w	Time (h)	Conversion (%)	Selectivity (%)
—	0	12	8.26	22.8
—	0	24	10.3	28.9
GO	1	12	75.1	54.9
GO	1	24	81.4	61.4
GO	10	12	83.3	68.8
GO	10	24	88.2	75.4
GO	20	24	96.3	88.1
<b>ZnO</b>	<b>1</b>	<b>12</b>	<b>50.9</b>	<b>49.2</b>
<b>ZnO</b>	<b>1</b>	<b>24</b>	<b>49.8</b>	<b>50.3</b>
<b>ZnO</b>	<b>10</b>	<b>12</b>	<b>56.3</b>	<b>47.6</b>
<b>ZnO</b>	<b>10</b>	<b>24</b>	<b>59.6</b>	<b>57.1</b>
GO/ZnO	1	12	95.9	71.2
GO/ZnO	1	24	96.3	73.8
GO/ZnO	10	12	98.4	85.4
GO/ZnO	10	24	98.6	89.5

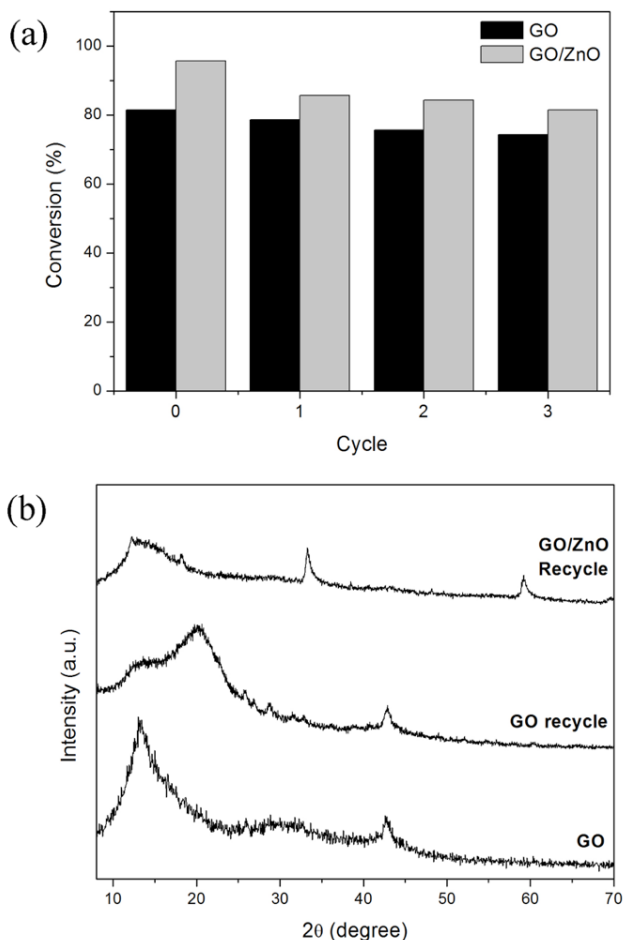


**Figure 9.** (a) Recycle reactions of ring-opening of epoxidized soybean FAME using GO and GO/ZnO catalysts and (b) XRD patterns of GO and GO/ZnO after recycling reactions comparing with GO before reaction.

from the composite, resulting in a reduction of 11% in the reaction yield upon the third recycle. Noteworthy, these results are similar to those presented by GO (reaction yield of *ca.* 10 %) under the same recycle regime. Thus, the heterogeneous acid catalysts herein presented were not deactivated during the acetylation reaction, presenting excellent activity/cycle, thermal stability around 120 °C and water tolerance. In addition, both heterogeneous catalysts can be easily separated from the reaction medium.

## CONCLUSIONS

GO and the GO/ZnO nanocomposite were synthesized, characterized and used as a heterogeneous catalytic system for the acetylation of soybean FAME. Indeed, GO and GO/ZnO were active for epoxy ring-opening with acetic anhydride, achieving great conversion rates and selectivity. The best results were obtained at 120 °C for 24 h. The GO/ZnO nanocomposite showed better performance than GO

catalyst and the selectivity was enhanced when the amount of catalyst was increased. The epoxy ring was almost completely opened in the presence of GO or GO/ZnO nanocomposite and partially opened using only ZnO as catalysts, with conversion up to *ca.* 99% and selectivity of *ca.* 90%, showing that the proposed reaction could be easily performed using GO or GO/ZnO catalysts. The catalytic activities in all recycle reactions were practically preserved with activities up to 85%. Although the activity of GO/ZnO catalyst decreased, probably due to the ZnO nanoparticle leaching, the GO catalyst showed stable catalytic activity and does not undergo deactivation during the acetylation reaction. Therefore, the GO and GO/ZnO heterogeneous catalysts present good conversion and selectivity for epoxy ring-opening in the acetylation reaction of epoxide soybean FAME with ease of separation, excellent activity, thermal stability at 120 °C, being great catalysts for these reactions.

## ACKNOWLEDGMENTS

Authors acknowledge CAPES, CNPq and FAP-DF for financial support and fellowships.

## REFERENCES

- Acocella, M.R., Corcione, C.E., Giuri, A., Maggio, M., Maffezzoli, A., Guerra, G. Graphene oxide as a catalyst for ring opening reactions in amine crosslinking of epoxy resins. *RSC Adv.*, 6, 23858-23865 (2016). <https://doi.org/10.1039/C6RA00485G>
- Aerts, H.A.J., Jacobs, P.A. Epoxide yield determination of oils and fatty acid methyl esters using <sup>1</sup>H NMR. *J. Am. Oil Chem. Soc.*, 81, 841-846 (2004). <https://doi.org/10.1007/s11746-004-0989-1>
- Anthrop, D.F., Searcy, A.W. Sublimation and Thermodynamic Properties of Zinc Oxide. *J. Phys. Chem.*, 68, 2335-2342 (1964). <https://doi.org/10.1021/j100790a052>
- Araújo, J.V.D.S., Ferreira, R.V., Yoshida, M.I., Pasa, V.M.D. Zinc nanowires synthesized on a large scale by a simple carbothermal process. *Solid State Sci.*, 11, 1673-1679 (2009). <https://doi.org/10.1016/j.solidstatesciences.2009.05.034>
- Azeh, Y., Olatunji, G.A., Mohammed, C., Mamza, P.A. Acetylation of wood flour from four wood species grown in Nigeria using vinegar and acetic anhydride. *Int. J. Carbohydr. Chem.*, 2013, 1-6 (2013). <https://doi.org/10.1155/2013/141034>
- Bian, J., Xiao, M., Wang, S., Wang, X., Lu, Y., Meng, Y. Highly effective synthesis of dimethyl carbonate from methanol and carbon dioxide using a novel copper-nickel/graphite bimetallic nanocomposite catalyst. *Chem. Eng. J.*, 147, 287-296 (2009a). <https://doi.org/10.1016/j.cej.2008.11.006>

- Bian, J., Xiao, M., Wang, S.J., Lu, Y.X., Meng, Y.Z. Graphite oxide as a novel host material of catalytically active Cu-Ni bimetallic nanoparticles. *Catal. Commun.*, 10, 1529-1533 (2009b). <https://doi.org/10.1016/j.catcom.2009.04.009>
- Biresaw, G., Bantchev, G.B. Tribological properties of biobased ester phosphonates. *J. Am. Oil Chem. Soc.*, 90, 891-902 (2013). <https://doi.org/10.1007/s11746-013-2232-1>
- Campanella, A., Fontanini, C., Baltanás, M.A. High yield epoxidation of fatty acid methyl esters with performic acid generated in situ. *Chem. Eng. J.*, 144, 466-475 (2008). <https://doi.org/10.1016/j.cej.2008.07.016>
- Carvalho, M.S., Mendonça, M.A., Pinho, D.M.M., Resck, I.S., Suarez, P.A.Z. Chromatographic analyses of fatty acid methyl esters by HPLC-UV and GC-FID. *J. Braz. Chem. Soc.*, 23, 763-769 (2012). <https://doi.org/10.1590/S0103-50532012000400023>
- Cheng, J., Qiu, Y., Huang, R., Yang, W., Zhou, J., Cen, K. Biodiesel production from wet microalgae by using graphene oxide as solid acid catalyst. *Bioresour. Technol.*, 221, 344-349 (2016). <https://doi.org/10.1016/j.biortech.2016.09.064>
- Dhakshinamoorthy, A., Alvaro, M., Concepción, P., Fornés, V., Garcia, H. Graphene oxide as an acid catalyst for the room temperature ring opening of epoxides. *Chem. Commun.*, 48, 5443-5445 (2012). <https://doi.org/10.1039/c2cc31385e>
- Diciccio, A.M., Coates, G.W. Ring-opening copolymerization of maleic anhydride with epoxides: A chain-growth approach to unsaturated polyesters. *J. Am. Chem. Soc.*, 133, 10724-10727 (2011). <https://doi.org/10.1021/ja203520p>
- Dreyer, D.R., Jia, H.P., Bielawski, C.W. Graphene oxide: A convenient carbocatalyst for facilitating oxidation and hydration reactions. *Angew. Chemie - Int. Ed.*, 49, 6813-6816 (2010). <https://doi.org/10.1002/anie.201002160>
- Gao, Y., Ma, D., Wang, C., Guan, J., Bao, X. Reduced Graphene Oxide as Catalyst for Hydrogenation of Nitrobenzene. *Chem. Commun.*, 47, 2432-2434 (2011). <https://doi.org/10.1039/C0CC04420B>
- Garg, B., Bisht, T., Ling, Y.C. Graphene-based nanomaterials as heterogeneous acid catalysts: A comprehensive perspective. *Molecules*, 19, 14582-14614 (2014). <https://doi.org/10.3390/molecules190914582>
- Guo, Y., Chang, B., Wen, T., Zhao, C., Yin, H., Zhou, Y., Wang, Y., Yang, B., Zhang, S. One-pot synthesis of graphene/zinc oxide by microwave irradiation with enhanced supercapacitor performance. *RSC Adv.*, 6, 19394-19403 (2016). <https://doi.org/10.1039/C5RA24212F>
- Huang, Z., Liu, G., Kang, F. Glucose-Promoted Zn-Based Metal – Organic Framework / Graphene Oxide Composites for Hydrogen Sul fi de Removal. *ACS Appl. Mater. Interfaces*, 4, 4942-4947 (2012). <https://doi.org/10.1021/am3013104>
- Hummers, W.S., Offeman, R.E. Preparation of Graphitic Oxide. *J. Am. Chem. Soc.*, 80, 1339 (1958). <https://doi.org/10.1021/ja01539a017>
- Jacinto, G.V.M., Brolo, A.G., Corio, P., Suarez, P. a Z., Rubim, J.C. Structural Investigation of MFe<sub>2</sub>O<sub>4</sub> (M = Fe, Co) Magnetic Fluids. *J. Phys. Chem. C*, 113, 7684-7691 (2009). <https://doi.org/10.1021/jp9013477>
- Jia, H.P., Dreyer, D.R., Bielawski, C.W., C-H oxidation using graphite oxide. *Tetrahedron*, 67, 4431-4434 (2011). <https://doi.org/10.1016/j.tet.2011.02.065>
- Joonwichien, S., Yamasue, E., Okumura, H., Ishihara, K.N. Effect of Static Magnetic Field on Photocatalytic Degradation of Methylene Blue over ZnO and TiO<sub>2</sub> Powders. *Appl. Magn. Reson.*, 42, 17-28 (2012). <https://doi.org/10.1007/s00723-011-0270-0>
- Li, B., Liu, T., Wang, Y., Wang, Z. ZnO/graphene-oxide nanocomposite with remarkably enhanced visible-light-driven photocatalytic performance. *J. Colloid Interface Sci.*, 377, 114-121 (2012). <https://doi.org/10.1016/j.jcis.2012.03.060>
- Madankar, C.S., Dalai, A.K., Naik, S.N. Green synthesis of biolubricant base stock from canola oil. *Ind. Crops Prod.*, 44, 139-144 (2013). <https://doi.org/10.1016/j.indcrop.2012.11.012>
- Marso, T.M.M., Kalpage, C.S., Udugala-Ganehenege, M.Y. Metal modified graphene oxide composite catalyst for the production of biodiesel via pre-esterification of *Calophyllum inophyllum* oil. *Fuel*, 199, 47-64 (2017). <https://doi.org/10.1016/j.fuel.2017.01.004>
- McNutt, J., He, Q.S. Development of biolubricants from vegetable oils via chemical modification. *J. Ind. Eng. Chem.*, 36, 1-12 (2016). <https://doi.org/10.1016/j.jiec.2016.02.008>
- Min, S., Lu, G. Dye-sensitized reduced graphene oxide photocatalysts for highly efficient visible-light-driven water reduction. *J. Phys. Chem. C*, 115, 13938-13945 (2011). <https://doi.org/10.1021/jp203750z>
- Moharram, A.H., Mansour, S.A., Hussein, M.A., Rashad, M. Direct precipitation and characterization of ZnO nanoparticles. *J. Nanomater.*, 2014, 20-25 (2014). <https://doi.org/10.1155/2014/716210>
- Nasrollahzadeh, M., Jaleh, B., Jabbari, A. Synthesis, characterization and catalytic activity of graphene oxide/ZnO nanocomposites. *RSC Adv.*, 4, 36713-36720 (2014). <https://doi.org/10.1039/C4RA05833J>

- Navalón, S., Herance, J.R., Álvaro, M., García, H. General aspects in the use of graphenes in catalysis. *Mater. Horizons*, 5, 363-378 (2018). <https://doi.org/10.1039/C8MH00066B>
- Nicolau, A., Samios, D., Piatnick, C.M.S., Reiznaut, Q.B., Martini, D.D., Chagas, A.L. On the polymerisation of the epoxidised biodiesel: The importance of the epoxy rings position, the process and the products. *Eur. Polym. J.*, 48, 1266-1278 (2012). <https://doi.org/10.1016/j.eurpolymj.2012.04.013>
- Nie, Y., Wang, W.N., Jiang, Y., Fortner, J., Biswas, P. Crumpled reduced graphene oxide-amine-titanium dioxide nanocomposites for simultaneous carbon dioxide adsorption and photoreduction. *Catal. Sci. Technol.*, 6, 6187-6196 (2016). <https://doi.org/10.1039/C6CY00828C>
- Oliveira, J.S., Montalvão, R., Daher, L., Suarez, P.A.Z., Rubim, J.C. Determination of methyl ester contents in biodiesel blends by FTIR-ATR and FTNIR spectroscopies. *Talanta*, 69, 1278-1284 (2006). <https://doi.org/10.1016/j.talanta.2006.01.002>
- Oliveira, R.S., Machado, P.M.A., Ramalho, H.F., Rangel, E.T., Suarez, P.A.Z. Acylation of epoxidized soybean biodiesel catalyzed by SnO/Al<sub>2</sub>O<sub>3</sub> and evaluation of physical chemical and biologic activity of the product. *Ind. Crops Prod.*, 104, 201-209 (2017). <https://doi.org/10.1016/j.indcrop.2017.04.049>
- Ramalho, H.F., Di Ferreira, K.M.C., Machado, P.M.A., Oliveira, R.S., Silva, L.P., Prauchner, M.J., Suarez, P.A.Z. Biphasic hydroformylation of soybean biodiesel using a rhodium complex dissolved in ionic liquid. *Ind. Crops Prod.*, 52, 211-218 (2014). <https://doi.org/10.1016/j.indcrop.2013.10.023>
- Ruschel, C.F.C., Ferrão, M.F., Santos, F.P. dos, Samios, D. Otimização do Processo de Transesterificação em Duas Etapas para produção de biodiesel. *Quím. Nova*, 39, 267-272 (2016).
- Sakthivel, T.S., Das, S., Pratt, C.J., Seal, S. One-pot synthesis of a ceria-graphene oxide composite for the efficient removal of arsenic species. *Nanoscale*, 9, 3367-3374 (2017). <https://doi.org/10.1039/C6NR07608D>
- Samper, M.D., Fombuena, V., Boronat, T., García-Sanoguera, D., Balart, R. Thermal and mechanical characterization of epoxy resins (ELO and ESO) cured with anhydrides. *J. Am. Oil Chem. Soc.*, 89, 1521-1528 (2012). <https://doi.org/10.1007/s11746-012-2041-y>
- Scala, J. La, Wool, R.P. The effect of fatty acid composition on the acrylation kinetics of epoxidized triacylglycerols. *J. Am. Oil Chem. Soc.*, 79, 59-63 (2002). <https://doi.org/10.1007/s11746-002-0435-4>
- Sharma, R.V., Dalai, A.K. Synthesis of biolubricant from epoxy canola oil using sulfated Ti-SBA-15 catalyst. *Appl. Catal. B Environ.*, 142, 604-614 (2013). <https://doi.org/10.1016/j.apcatb.2013.06.001>
- Sharma, R.V., Somidi, A.K.R., Dalai, A.K. Preparation and properties evaluation of biolubricants derived from canola oil and canola biodiesel. *J. Agric. Food Chem.*, 63, 3235-3242 (2015). <https://doi.org/10.1021/jf505825k>
- Sheng, Y., Tang, X., Peng, E., Xue, J. Graphene oxide based fluorescent nanocomposites for cellular imaging. *J. Mater. Chem. B*, 1, 512-521 (2013). <https://doi.org/10.1039/C2TB00123C>
- Wang, A., Chen, L., Jiang, D., Yan, Z. Vegetable oil-based ionic liquid microemulsions and their potential as alternative renewable biolubricant basestocks. *Ind. Crops Prod.*, 51, 425-429 (2013). <https://doi.org/10.1016/j.indcrop.2013.09.039>
- Wang, H., Deng, T., Wang, Y., Cui, X., Qi, Y., Mu, X., Hou, X., Zhu, Y. Graphene oxide as a facile acid catalyst for the one-pot conversion of carbohydrates into 5-ethoxymethylfurfural. *Green Chem.*, 15, 2379-2383 (2013). <https://doi.org/10.1039/c3gc41109e>
- Wang, J., Li, H., Zhang, R., Shi, X., Yi, J., Wang, J., Huang, Q., Yang, W. Highly active copolymerization of ethylene and N-acetyl-O-( $\omega$ -alkenyl)-L-tyrosine ethyl esters catalyzed by titanium complex. *Polymers (Basel)*, 8, 1-12 (2016). <https://doi.org/10.3390/polym8030064>
- Zhang, Q., He, Y.Q., Chen, X.G., Hu, D.H., Li, L.J., Yin, T., Ji, L.L. Structure and photocatalytic properties of TiO<sub>2</sub>-Graphene Oxide intercalated composite. *Chinese Sci. Bull.*, 56, 331-339 (2011). <https://doi.org/10.1007/s11434-010-3111-x>

